CEFC2008 CD.PDF - Adobe Acrobat Pro

파일(F) 편집(E) 보기(V) 문서(D) 주석(C) 양식(R) 도구(T) 고급(A) 창(W) 도움말(H)

작성 결합 공동 작업 보안 서명 양식 멀티미디어 주석

a 1/680 78.1% 찾기

13TH IEEE CEFC 2008

Athens, 11-15 May 2008

Booklet

Program

Digests

Authors' Index by Page

Authors' Index by Session

Search

PD5 – Coupled Problems II FOYER

Tuesday, May 13th

13:40 – 15:20 Session Chair: **F. Morabito, C. Antonopoulos**

Torque Ripple Reduction Considering Magnetic Saturation in Permanent Magnet Synchronous Motor for EPS Application

Geun-Ho Lee, Suk-Hee Lee, Sung-Il Kim, Jung-Pyo Hong, *Senior Member, IEEE*
School of Mechanical Engineering, Hanyang University, Seoul 133-791, Korea

This paper deals with a novel method to reduce torque ripple of a permanent magnet synchronous motor (PMSM) for electric power steering (EPS) system. Such an application requires very low torque ripple in order to maintain good steering feel. However, because of spatial limitation, it can't help having the partial saturation in the iron core of the PMSM for the EPS, and the saturation results in significant torque ripple. Therefore, this paper analyzes torque ripple caused by the magnetic saturation of the PMSM and proposes a method concerning inductance measurement to verify the partial saturation. Also, it is shown that the compensation current is required in order to minimize torque ripple when the PMSM is driving at the high torque region, and the estimation process of the current and torque ripple decreased by the current are presented and verified with test result.

***Index Terms*—Electric power steering, magnetic saturation, permanent magnet synchronous motor, torque ripple.**

I. INTRODUCTION

ELECTRIC power steering (EPS) is a system that supplies motor power directly to the steering in order to assist steering torque. Compared to a conventional hydraulic Power Steering (HPS), of which an oil pump is always driven by the engine, the EPS contributes positively to the environment through improving fuel economy, reducing CO_2 emissions and eliminating waste oil. Thus, the HPS is increasingly replacing with the EPS [1], [2].

A permanent magnet synchronous motor (PMSM) has been applied for the performance improvement of EPS. Because the PMSM has many advantages such as high efficiency and high torque per rotor volume, it is especially suitable for automotive application where space and energy savings is critical.

In the column typed EPS system, the PMSM is connected to the steering shaft via a reduction gear, so the motor vibration and torque fluctuation are directly transferred through the steering wheel to the hands of a driver. For that reason, only the ripple between one and three percent of rated torque is permitted. There are a lot of technical papers that have presented the motor design and control technique to reduce cogging torque and torque pulsation [3]-[6]. However, unlike them, this paper shows the estimation method of compensation current for suppressing torque ripple caused by the magnetic saturation in the PMSM.

Due to the spatial limitation in the EPS application, the magnetic saturation in the stator core is inevitable in high torque region. This paper analyzes torque ripple generated by the partial saturation in the motor fabricated for the EPS. Furthermore, d-axis inductance is measured to prove the saturation with the use of discrete fourier transform (DFT). The harmonic current distribution which must be added to q-axis current to minimize torque ripple is calculated through finite element analysis (FEA), and the effective method in the PMSM driver is proposed in order to create the harmonic current. In the end, the results are verified by test.

Digital Object Identifier inserted by IEEE

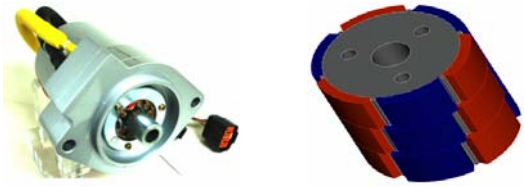

(a) Assembly of PMSM (b) Rotor configuration

Fig. 1. PMSM fabricated for the column typed EPS.

II. PMSM FOR THE EPS SYSTEM

A. Characteristics of PMSM for the EPS

Fig. 1 shows a fabricated PMSM for the column typed EPS system and the rotor configuration skewed in order to reduce cogging torque. The dimension and specification of PMSM are listed in Table I, and cogging torque and total harmonic distortion (THD) of back-EMF required in the motor is less than 0.02Nm and 0.7% respectively. Fig. 2 displays the torque waveforms when the PMSM is driven with constant q-axis current. To measure torque ripple accurately, the motor is driven at 10rpm, and input current is controlled with THD less than 0.5%. The 6 times torque ripple of electric frequency is increased as the magnetic torque is higher. Therefore, even if it has good characteristics in the low torque region, the torque ripple generated at the rated torque can't be neglected.

B. Inductance Measurement of PMSM

In this section, an inductance measurement method is presented in order to demonstrate the magnetic saturation effect of PMSM. The effect can be observed from the stator winding terminals as the change of inductance. The inductance depends on the input current and the rotor position. The measurement of inductance is accomplished by using DFT with high frequency current injection and discussed in the following.

The equivalent circuit for the vector control of PMSM is based on a synchronously rotating reference frame, and the mathematical model of equivalent circuit is given as follow:

TABLE I
DIMENSION AND SPECIFICATION OF PMSM

Items	Value
Stator outer diameter	117.2 mm
Rotor outer diameter	70.8 mm
Br (@20~25°C)	1.35 T
Number of poles and slots	6 / 9
Rated torque	4 Nm
Rated current	70 A_{rms}
Base and Maximum speed	1000, 2000 rpm

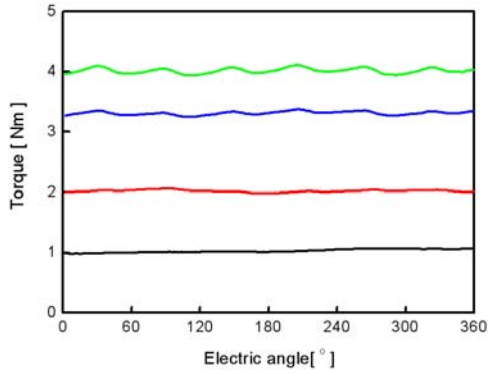

Fig. 2. Torque waveforms of PMSM measured at 10rpm.

$$\begin{bmatrix} v_d \\ v_q \end{bmatrix} = \begin{bmatrix} R_s + pL_d & -\omega_s L_q \\ \omega_s L_d & R_s + pL_q \end{bmatrix} \begin{bmatrix} i_d \\ i_q \end{bmatrix} + \begin{bmatrix} 0 \\ \omega_s \psi_a \end{bmatrix} \begin{bmatrix} i_d \\ i_q \end{bmatrix} \quad (1)$$

where i_d, i_q: d, q components of armature current; v_d, v_q: d, q components of terminal voltage; ψ_a: $\sqrt{3/2}\,\psi_f$; ψ_f: maximum flux linkage of permanent magnet; R_a: armature winding resistance; L_d, L_q: inductance along d-, q-axis; $p = d/dt$; P_n: number of pole pairs.

The saturation phenomenon occurs in all three phases and can be transformed to the orthogonal d-q coordinates oriented toward a desired direction determined by the angle (θ). A high frequency alternating current is injected in the synchronously rotating frame, and the inductance is measured at each angle when PMSM is rotating. The d-axis behaves just as a resistance and inductance.

$$\frac{V_{dac}(\omega)}{I_{dac}(\omega)} = R + j\omega L_d \quad (3)$$

$$\omega L_d = imag\left\{\frac{V_{dac}(\omega)}{I_{dac}(\omega)}\right\} \quad (4)$$

$$X(\omega_o) = \frac{1}{N}\sum_{n=0}^{N-1} x(nT_s)\cdot e^{-j\omega_o nT_s} = a_1 - jb_1 \quad (5)$$

To measure the d-axis inductance at a given angle, the axis is excited with a periodic small signal having frequency ω_o and sampled N times per period. The value of commanded voltage and feedback current are measured at the excitation frequency of the small signal by using DFT. The inductance is calculated from the voltage and current coefficients after one or several periods of small signal excitation.

$$a_1 = \frac{1}{N}\sum_{n=0}^{N-1} x(nT_s)\cdot\cos\left(\omega_o nT_s\right) \quad (6)$$

$$b_1 = \frac{1}{N}\sum_{n=0}^{N-1} x(nT_s)\cdot\sin\left(\omega_o nT_s\right) \quad (7)$$

$$L_d = \frac{1}{\omega_o}\frac{a_{1Vd}\times b_{1Id} - a_{1Id}\times b_{1Vd}}{a_{1Id}^2 + b_{1Id}^2} \quad (8)$$

where a_{1Id} and a_{1Vd} are the fourier coefficient of current and voltage. Fig. 3 shows the block diagram of inductance measurement which has the high frequency current reference, BPF and DFT block in the vector controller.

The three percent of rated current with 500Hz are injected and I_{de} and V_{de} signals are filtered by BPF when the motor is running at low speed. D-axis inductance is decreased according to d-axis current increases, and it has 6 times fluctuation of electric frequency as shown in Fig. 4. We can find that the partial saturation of stator teeth makes 6 times torque ripple of electric frequency in the PMSM.

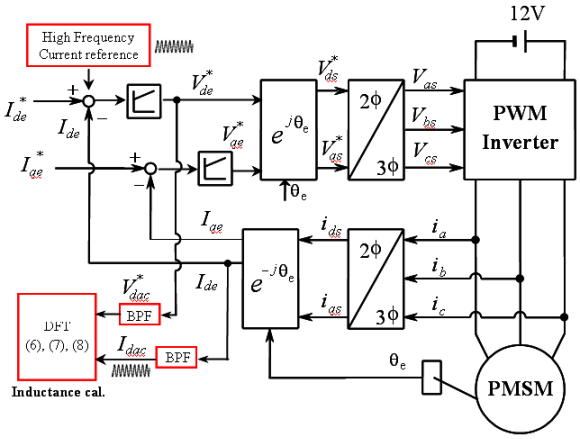

Fig. 3. Inductance measurement block diagram at vector control.

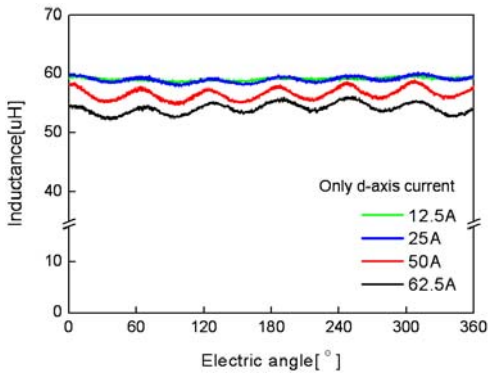

Fig. 4. D-axis inductance distribution according to electric angle.

III. Estimation Process of Compensation Current

In this paper, FEA is used in order to analyze the characteristics of PMSM and get the waveform of injection current to reduce torque pulsation. Nonlinear analysis considers the magnetic saturation of stator core. Fig. 5 shows the flux density distribution, and the maximum flux density of stator teeth indicates 2.2T at the rated current.

As shown in Fig. 6, the torque characteristics of PMSM are obtained by FEA, and the analysis result is compared to experimental result. The result at the rated current is similar to experimental result. In the test, the PMSM is rotated at low speed in order to drive the motor with a sinusoidal current. In this paper, the flow chart displayed in Fig. 7 is employed in order to obtain q-axis current distribution which minimizes torque ripple according to electric angle θ_e. FEA is iterated at the each rotor position with varying I_{qAC} to search the flat torque waveform.

$$i_q = i_{q0} + i_{qAC} \tag{9}$$

where i_{q0}: q component of armature current for the rated torque; i_{qAC}: compensation current added to i_{q0} in order to minimize torque ripple.

From this method, the compensation current which can minimize torque fluctuation is calculated according to current angle and expressed like Fig. 8. At the rated torque, 2.5A peak current is added to q-axis current.

IV. A Strategy To Minimize Torque Ripple and Test Results

The compensation current according to a given torque is obtained like Fig. 9 while d-axis current is controlled to zero. As shown in Fig. 10, the harmonics of compensation current displayed in Fig. 9 consist of 6th, 12th, 18th and 24th harmonic component according to q-axis current. Therefore, if 18th and 24th harmonic component is neglected, the current can be simplified as the function of i_{q0}:

$$\begin{aligned} i_{qAC} = &\sqrt{0.062 + 0.00028 i_{q0}^{\,2}} \cdot \cos(6\theta_e) \\ &+ (0.071 + 0.0056 i_{q0}) \cdot \cos(12\theta_e) \end{aligned} \tag{10}$$

Fig. 11 shows the effective real time compensation strategy to minimize torque ripple caused by magnetic saturation in the vector controller. In the Table II, the experimental equipment is briefly shown. The most recent digital signal processor, TMX320F28335 of Texas Instrument, is employed in order to drive the motor. Because of very low inductance, we choose 20kHz switching frequency to minimize high frequency current ripple. From the test result, the 6 times torque harmonic of electric frequency is decreased to 30% as shown in Fig.12. By injecting the only 2% current of rated current, torque ripple caused by the partial saturation could be effectively suppressed.

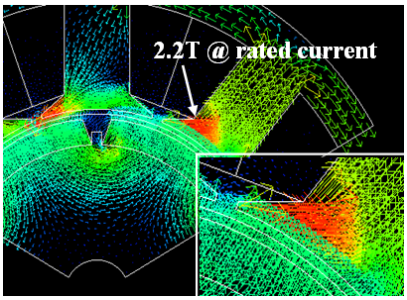

Fig. 5. Flux density distribution at 70A.

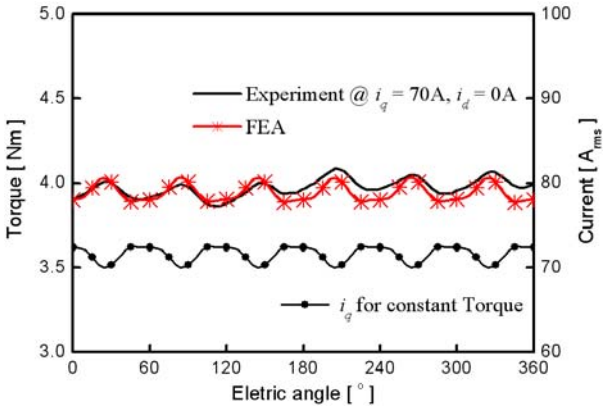

Fig. 6. Torque comparison of analysis and test result.

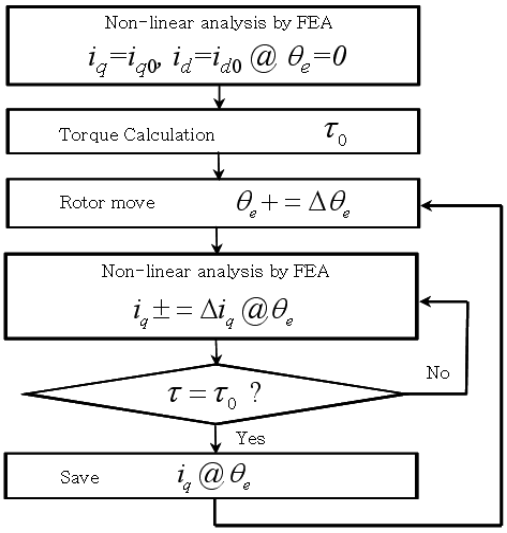

Fig. 7. Estimation procedure of the compensation current.

V. Conclusion

In this paper, an effective real time inductance measurement method using DFT was presented to obtain the inductance distribution according to the rotor position. This measurement method was used in order to prove the magnetic saturation of PMSM. Moreover, the saturation effect was analyzed by a nonlinear analysis, and the simple compensation strategy to minimize the torque ripple at each electric angle was proposed. Finally, the validity of the analysis and compensation method

was verified by test result of PMSM fabricated for the EPS, and with the method, the torque ripple caused by the magnetic saturation could be effectively reduced at the rated torque.

REFERENCES

[1] Y. Shimizu and T. Kawai, "Development of Electric Power Steering," *SAE Transactions*, no. 1991-0014, 1991.

[2] N. Bianchi, M. D. Pre, and S. Bolognani, "Design of a fault-tolerant IPM motor for electric power steering," *IEEE Trans. Veh. Technol*., vol. 55, no. 4, pp. 1102-1111, July 2006.

[3] M. S. Islam, S. Mir, T. Sebastian, and S. underwood, "Design considerations of sinusoidally excited permanent-magnet machaines for low-torque-ripple applications," *IEEE Trans. Ind. Applicat*., vol. 41, no. 4, pp. 955-962, July 2005.

[4] P. Mattavelli, L. Tubiana, and M. Zigliotto, "Torque-ripple reduction in PM synchronous motor drives using repetitive current control," *IEEE Trans. Poewer Electron*., vol. 20, no. 6, pp. 1423-1431, Nov. 2005.

[5] N. Bianchi and S. Bolognani, "Design techniques for reducing the cogging torque in surface-mounted PM motors," *IEEE Trans. Ind. Applicat.*, vol. 38, no. 5, pp. 1259-1265, Sept./Oct. 2002.

[6] G. H. Lee, S. I. Kim, J. P. Hong, and J. H. Bhan, "Torque ripple reduction of interior permanent magnet synchronous motor using harmonic injected current," *IEEE Trans. Magn*., to be published.

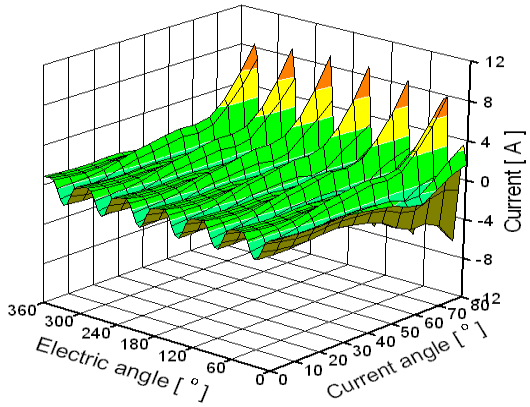

Fig. 8. Compensation current distribution according to current angle.

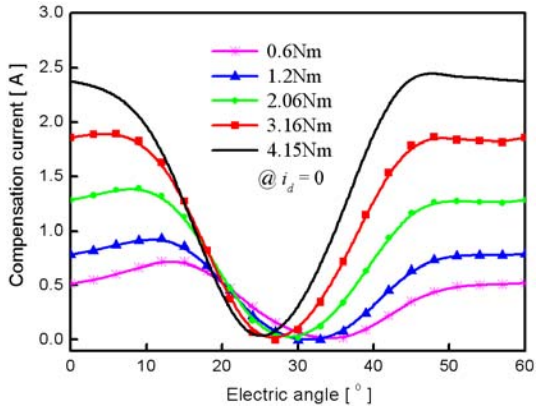

Fig. 9. Compensation current distribution according to a given torque.

TABLE V
OPTIMAL CONDITION

Items	Value
Switching Frequency	20 kHz
DSP	TMX320F28335
Power Switch	MOS FET - GWM 220-004
Torque Transducer	HBM –T34FN
DC link voltage	12 V

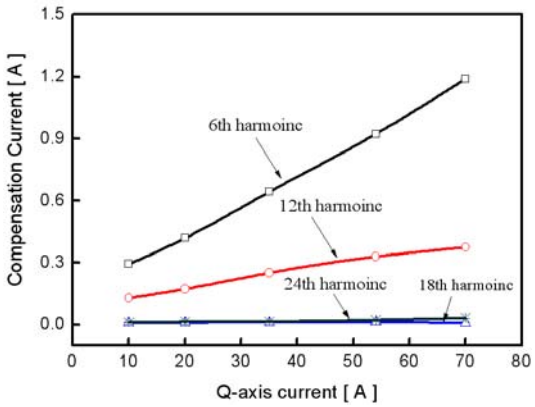

Fig. 10. Harmonic components of compensation current.

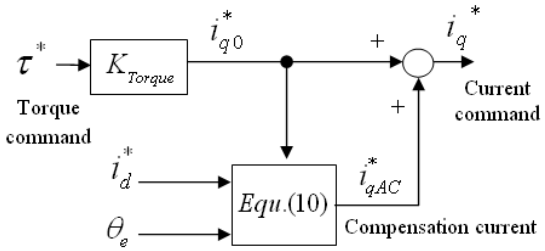

Fig. 11. Compensation strategy in the vector controller.

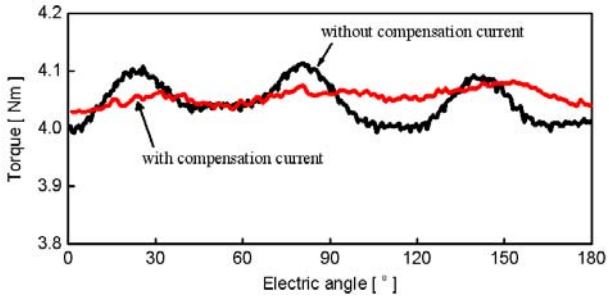

Fig. 12. Torque waveform at 70A.